



Electrodialysis performance during the defluoridation of brackish water using CINH2 membrane

Walid Mabrouk*, Ridha Lafi, Amor Hafiane

CERTE, Laboratory Water, Membranes and Biotechnology of the Environment, Soliman 8020, Tunisia, Tel. +216 53 30 43 24; email: w.mabroukfst@gmail.com (W. Mabrouk), Tel. +216 97 78 61 84; email: ridha.lafi@yahoo.fr (R. Lafi), Tel. +216 98 93 49 68; email: amor.hafiane@certe.rnrt.tn (A. Hafiane)

Received 29 January 2021; Accepted 15 July 2021

ABSTRACT

In the present work, we propose to investigate the fluoridation of brine water by electrodialysis using a new exchange membrane. This membrane called CINH2 was prepared by crosslinking chlorosulfonated polyethersulfone (SO₂Cl-PES) using aminated polyethersulfone (NH₂-PES) reagent. The efficiency of the electrodialysis process at different NaCl concentration ranging from 0.5 to 3.0 g/L was evaluated by the determination of demineralization rate, the ionic flux transport (*J*), the fluoride concentration on the dilute side and the specific power consumption. After defluoridation of the treated solutions, ions fluoride concentrations become lower than the amount fixed by the World Health Organization for drinking water. This study shows clearly that the electrodialysis process using the CINH2 membrane is very promising for the defluoridation of water.

Keywords: Proton exchange membrane; Electrodialysis; CINH2 membrane; Desalination; Fluoride removal; Brackish water; NaCl removal

1. Introduction

Electrodialysis (ED) is an electro-membrane process in which an electrical potential gradient is applied for the selective and recuperation of ions from solutions [1]. Ions are transported through ion-exchange membranes (IEMs) from the dilute to the concentrated tank. ED is a mature separation process applied mainly in water treatment and in the food industry because it is a robust, efficient and versatile method for such applications. The electrodialysis is largely used during the desalination of water and NaCl recovery from seawater [2,3].

The main core of the ED unit is composed of a membrane stack consisting of planar plate anion and cation membranes distributed in a sandwich form. Among the important components in the electrodialysis unit are the membranes. They have gained more attention in both academic and industry

due to their high ion exchange capacity toward specific ions in electrochemical applications in separation processes [4–7].

Ion-exchange membranes contain either fixed charged groups. Depending on the presence of positive or negative charged groups, these membranes are subdivided into anion (AEM) and cation exchange membranes (CEM), respectively. IEMs are selective for negative and positive charged ions and are very used in Chlor-alkali, diffusion dialysis and electrodialysis processes [8,9]. The ion exchange capacity of the membranes is an important parameter to compare the efficiency of IEMs in electro-membrane separation processes [10,11]. Thus, high conductivity, selectivity, thermochemical oxidative stability of IEMs have urgently been required for practical applications in the separation processes. In literature, several types of membranes have been described and show all these assets, for example, poly-

* Corresponding author.

ethersulfone (PES) [12], polystyrene (PS) [13], polyetherether ketone (PEEK) [14], and polyether benzimidazole (PBI) [15].

On the other hand, the presence of fluoride in water poses a health problem in many countries such as Tunisia. Indeed, fluoride ions are beneficial and necessary for the human organism but become toxic at a high level and cause problems to human health such as dental and skeleton fluorosis [16]. According to the latest estimates, about 200 million people around the world are under the dreadful problems of fluorosis [17]. The acceptable fluoride concentration on drinking water is under 1.5 mg/L according to the World Health Organization (WHO) [18].

The defluoridation of contaminated surface water and groundwater has been developed by various techniques such as adsorption [19], chemical precipitation [20], and electrocoagulation technologies [21]. Major shortcomings of these conventional technologies are the generation of large amounts of toxic sludge as secondary pollution and low effectiveness for removing trace fluoride contaminants. Membrane technology such as electrodialysis has the advantages of economic efficiency, high desalination capacity, and excellent selectivity [22]. ED process is particularly suitable for the removal of fluoride ions since this element is accompanied by high salinity [23,24].

In this work, we focus on chlorosulfonated polyethersulfone (Cl-PES), due to its excellent mechanical properties, and the high degree of sulfochloration up to 1.3 SO₂Cl group per monomer unit (pmu) [25,26]. SO₂Cl groups are very reactive and can be reacted with aminated groups of aminated polyethersulfone (NH₂-PES). Sulfochlorated PES and aminated PES have similar chemical structures that allow compatibility, and they are soluble and miscible in dimethylacetamide (DMAc) solvent [27,28]. Ion-conducting properties of sulfonated polyethersulfone polymers rely on proton solvation by water. Sufficient water uptake improves thus the membrane proton conductivity. The critical point of sulfonated polyethersulfone membranes remains, however, the mechanical properties: dry membranes are brittle and hydrate membranes may exhibit a dramatic loss of mechanical properties. A detailed description of the synthesis strategy of the CINH2 membrane has been described in previous works [27,28]. These membranes have shown excellent thermals, electrochemical properties, and good performances in PEMFC [27].

In this study, the CINH2 prepared membrane was applied for the removal of fluoride ions by electrodialysis from brackish polluted water with the usage of the stack containing CINH2/PC-SA assembly. The efficiency of this electro-membrane process is evaluated by the removal of fluoride rate, demineralization rate, ionic transport flux, and power consumption.

2. Experimental

2.1. Materials

Chlorosulfonated polyethersulfone and aminated polyethersulfone were synthesized by the author in ERAS Labo Enterprise in St. Nazaire les Eymes, Grenoble, France. N,N'-dimethylacetamide (DMAc) was purchased from Acros in Montoire sur le loir, France. Sodium hydroxide and sodium fluoride were purchased from Sigma-Aldrich in Saint-Louis, Missouri, United States. Cation exchange membrane (PC-SK) and anion exchange membrane (PC-SA) were purchased from PCCell GmbH German Enterprise.

2.2. Electrodialysis equipment

The electrodialysis configuration system consists of a current generator, a dilute, a concentrate, and an electrode rinse tank. Three centrifugal pumps are equipped each with a flow meter, and a valve to control the supply of feed flow rates in the compartments of ED cells [28,29].

The electrodialysis test was carried out using a laboratory stack (PCCell ED 64 002) which is composed of ion exchange membranes, spacers, and two electrodes. Both anode and cathode are made of Pt/Ir coated Titanium. The membranes and spacers are staked between the two electrode-end blocks. Plastic separators separate the membranes to train the blocks streams of the dilute and concentrate.

In the present work, the stack was equipped with two synthesized cation exchange membranes (CINH2) and two anion exchange membranes (PC-SA). The principles properties of membranes provided by the manufacturer are consigned in Table 1. An active surface of 64 cm² for each membrane was cut for use in the electrodialysis cell.

2.3. Experimental procedure and analytical methods

All experiments were carried for the electrodialysis stack used to treat brackish water by process batch mode at room temperature. The volume of dilute, concentrate and electrode rinse solution was 1 L. The same initial concentration of concentrate and dilute tanks was used (0.5, 1.5 and 3 g/L of NaCl). Before the experiments, the pH was adjusted by the addition of 1 M HCl and/or NaOH. 0.1 M Na₂SO₄ was used as electrode rinse solution circulating in electrode compartments, in order to prevent the generation of chlorine or hypochlorite, which could be hazardous for the electrodes. The flow rate of the electrode rinse solution was fixed to 80 L/h. The flow rate of dilute and concentrated compartments was fixed at the beginning of the experiment. The electrodialysis process was terminated when the dilute conductivity compartment can reach 0.3 mS/cm.

Table 1
Water uptake and ion exchange capacity of CINH2 membrane

Membrane	Thickness (μm)	Ion exchange capacity (meq/g)	Water uptake	Functional groups	Permselectivity
CINH2	120	2.2	40%	-SO ₃ ⁻	>0.93
PC-SA	130	1.5	10%	-HR ₄ ⁺	>0.96
PC-SK	130	2.2	14%	-SO ₃ ⁻	>0.99

In all experiments, the electrical conductivity (EC) of samples taken from the dilute and concentrate during each experiment was measured using a 712 Conductometer (Metrohm AG, Switzerland). Fluoride concentration was determined using ion-selective electrode in conjunction with a standard reference connected to a Metrohm 781 Ion Meter (Metrohm AG, Switzerland).

2.4. Membrane preparation

The protocol for the preparation of the CINH2 membrane was detailed in previous work [17]. Briefly, 0.2 mol equivalents of aminated polyethersulfone (NH₂-PES), the cross-linking agent, were reacted with (SO₂Cl) groups of chlorosulfonated PES. The crosslinking agent and sulfonated PES were dissolved separately at room temperature in dimethylacetamide at 10% in weight and mixed under-cooling. The resulting clear viscous polymer solution was stirred at low temperature, and casting on a Teflon plate and equitably distributed. Drying was carried out in an oven. After cooling, the resulting membrane was peeled off from Teflon. The thickness of the dry CINH2 membrane was about 100 μm. The chemical formula of the CINH2 membrane is presented in Fig. 1.

3. Characterization

3.1. Fourier-transform infrared spectroscopy

Fourier-transform infrared (FT-IR) spectrum of CINH2 membrane was conducted in transmission mode as a function of wavenumber using a Nicolet spectrophotometer (IR200 FT-IR) in the range of 400 to 4,000 cm⁻¹. The membrane sample was placed between the cast iron and

the diamond crystal (separator blade) without any prior preparation [40].

3.2. Morphology

Specimen for scanning electron microscopy (SEM) was prepared as a dry membrane sample. SEM observation (Quanta 650 FEG microscope) of the surface of the CINH2 membrane has been performed. Conditions were (50 s, 10 kV, 2,500 magnification and analyzed surface: 20 μm). Data were processed with the Pathfinder software. In addition, the chemical composition of the CINH2 membrane was determined by energy-dispersive X-ray (EDX) spectroscopy of a membrane area during SEM analysis.

3.3. Limiting current

In electro dialysis, the transport of charged species from the diluted compartment to the concentrated one was carried out across ion-exchange membranes. When the concentration of ion species increases on the membrane surface, the current density will approach the maximum value, called the limiting current density (LCD) [30]. The limiting current density of the electro dialysis process determines the current debited. When electro dialysis is operated at above LCD, it shows higher electrical resistance. It can give rise to problems such as salt precipitation. The determination of the LCD is necessary to operate the electro dialysis cell successfully [31].

The limiting current can be obtained by plotting the electrical resistance (E/I) against the reciprocal electrical current (1/I) [32]. This is called Cowan–Brown method. The resistance shows a sharp change in the resistance when the limiting current density is reached.

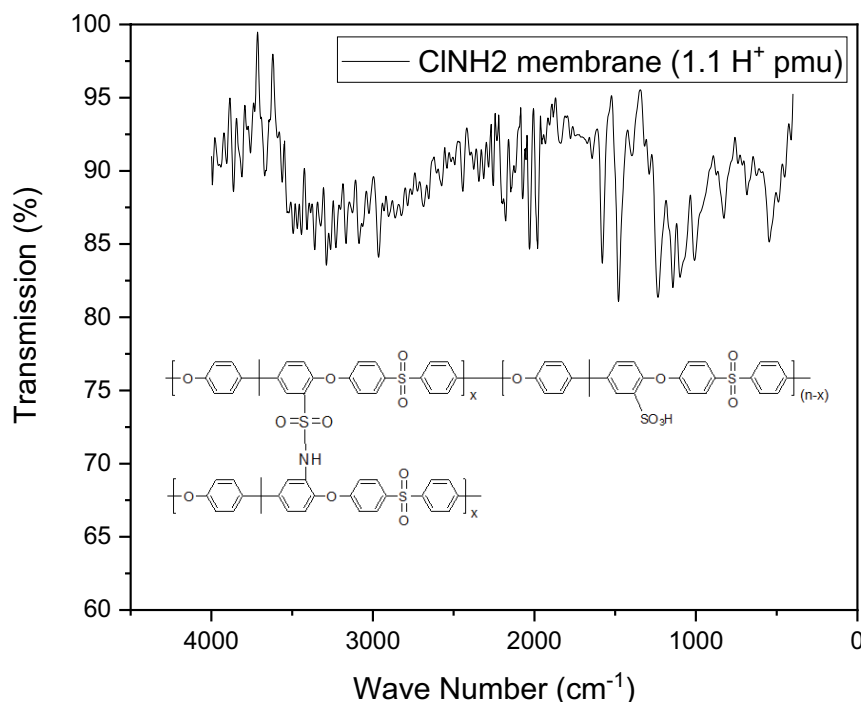


Fig. 1. FT-IR spectrum of CINH2 membrane.

3.4. Demineralization rate

Determination of demineralization rate (DR) was calculated as following [33]:

$$DR(\%) = 100 \left(1 - \frac{C_t^D}{C_0} \right) \quad (1)$$

where C_0 and C_t^D , expressed in S/cm, correspond to the initial and final conductivities of the dilute, respectively.

3.5. Ionic transport flux

The values of ionic transport flux from feed to the receiver phase were calculated for all experiments [34]. The ionic flux (J) was determined by using the following equation:

$$J(\text{mol cm}^{-2} \text{ s}^{-1}) = \left(\frac{V}{A} \right) \times \left(\frac{\Delta C}{\Delta t} \right) \quad (2)$$

where V is the volume of receiver phase (L), A is the effective membrane area (cm^2), ΔC is the transported amount of ions at a time (mol/L) and Δt is the period time (s).

3.6. Specific power consumption

The specific power consumption (SPC) can be described as the energy needed to treat 1 L of solution [35]. SPC was calculated using the following equation:

$$SPC(\text{W h L}^{-1}) = E \times \frac{\int_0^t I(t) dt}{V} \quad (3)$$

where E is the applied potential. I is the current. V is the dilute stream volume and t is the time.

3.7. Removal rate of fluoride ions

The removal rate of fluoride ions was calculated using the following [36]:

$$R_{f^-}(\%) = 100 \times \left(1 - \frac{C_t}{C_0} \right) \quad (4)$$

where C_t is fluoride concentration (mol/L) in the dilute compartment and C_0 is the initial concentration of fluoride in the feed phase (mol/L).

4. Results and discussions

4.1. FT-IR spectra

Fig. 1 shows the infrared spectrum of the synthesized CINH2 membrane with a high degree of sulfonation (1.1 proton pmu). Aromatic carbons can be seen as two strong bands around 1,480 and 1,583 cm^{-1} . Methyl groups appear with an absorption band around 1,243 cm^{-1} . The C–O–C appears around 1,142 cm^{-1} . The characteristic bands consistent at 1,098 and 1,008 cm^{-1} have been attributed to the symmetrical and asymmetrical stretching vibrations of the O=S=O grouping respectively, and those at 827 and 678 cm^{-1} are allied to the S–O vibrations and C–S, indicating the existence of sulfonic acid species in the samples analyzed. These bands prove the presence of the sulfonic group in the CINH2 membrane. The peaks at 3,400 and 2,964 cm^{-1} could be attributed to the hydrated O–H vibration in the membrane.

4.2. SEM observation and EDX analysis

The surface SEM analysis represented in Fig. 2 reveals the surface state of the synthesized CINH2 membrane. That micrograph just confirms the homogeneity of the fabricated CINH2 membrane and the absence of any cracks, holes or pores.

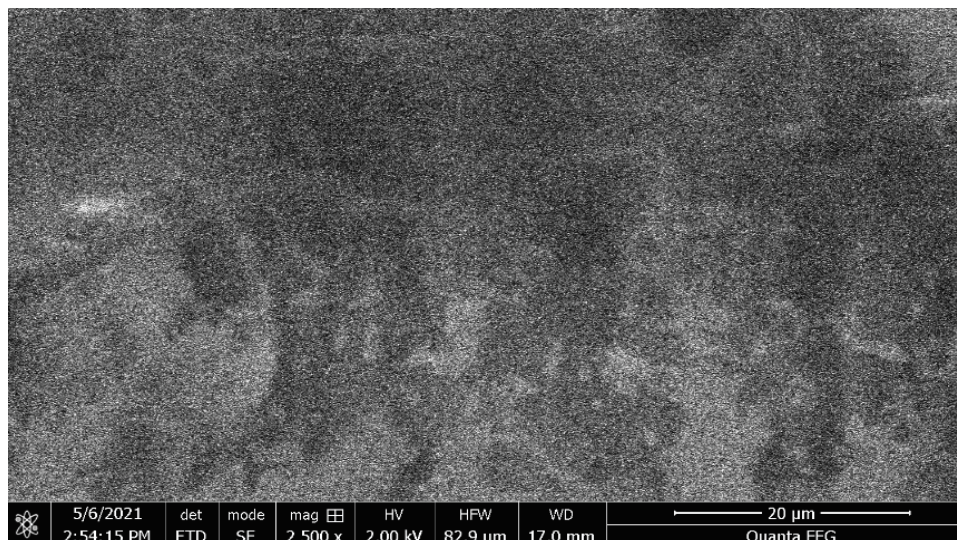


Fig. 2. Surface SEM image of CINH2 membrane.

EDX was further used to confirm the presence of the functionalized groups in the CINH2 membrane. Fig. 3 shows the different elements present in the synthesized membrane. Table 2 summarizes the percentages of all detectable elements present in the CINH2 membrane and the theoretical mass and weight percent of all elements. A difference between theoretical and experimental atomic and weight percent of different elements has been observed. EDX analysis of the CINH2 membrane remains a qualitative analysis.

4.3. Removal of fluoride from water

Fig. 4 shows the variation of electric resistance with the reciprocal electric current. These experiments were carried out with the feed solutions (0.5, 1.5 and 3.0 g/L NaCl), each containing 3.0 mg/L of fluoride, flowing into the dilute cell (DC) with a constant flow rate of 40 mL/min. The point at which the negative slope of the curve cuts the positive slope is designated as the opposite of limiting current according to Cowan and Brown's methods [30]. Furthermore,

the change of slope in the resistance curve can be due to water dissociation on the surface of the ion-exchange membrane [37].

The results of limiting current and debiting current of the CINH2/PC-SA assemblies are presented in Table 3. It is clear that the limiting current density decreases with the increase of the NaCl concentration. Also, a slight difference was observed between the limited currents and the debited current of the assemblies containing CINH2 membranes.

The removal of fluoride was studied at different sodium chloride solutions ranging from 0.5 to 3.0 g/L of sodium chloride and at a fixed fluoride concentration of 3.0 mg/L. The effects of NaCl concentration of the feed solution on the fluoride removal in terms of conductivity, demineralization rate, ionic flux, specific power consumption, and removal rate of fluoride ions have been investigated. An electrode overheating appeared in the present system using two anionic PC-SA membranes and two cationic CINH2 membranes when the initial concentration of feed solution was above 3 g/L. It is a result of the increase in cell conductivity.

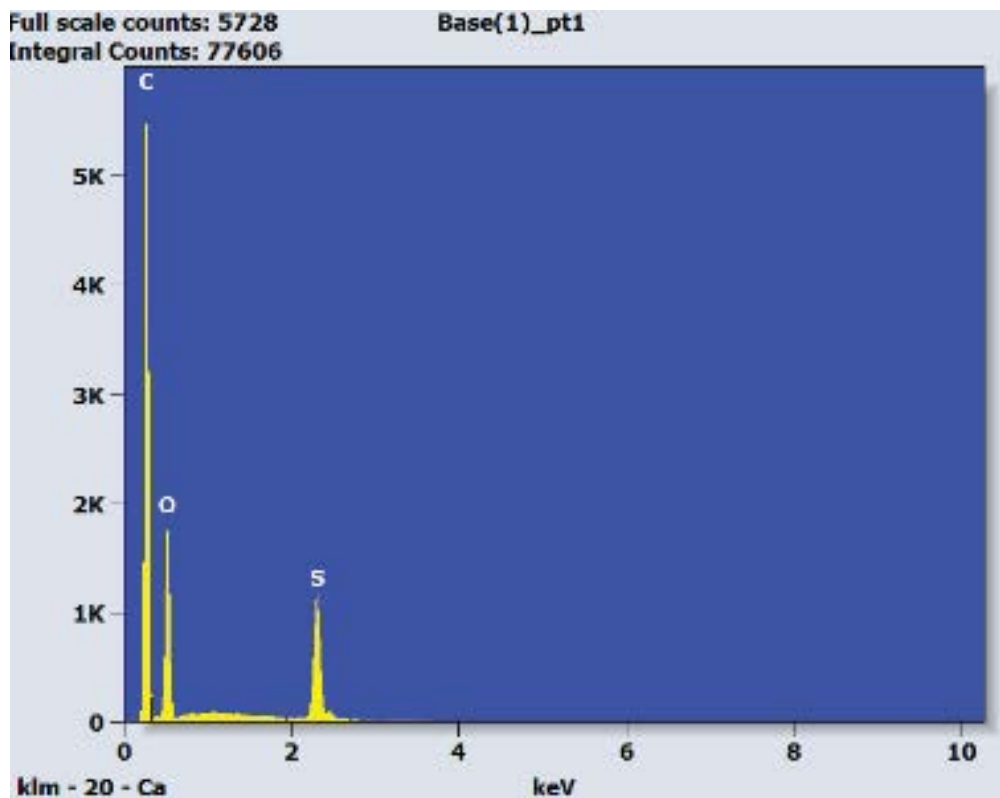


Fig. 3. Energy-dispersive X-ray spectrum of the synthesized membrane.

Table 2
Theoretical and experimental mass percent of elements in CINH2 membrane

Element	Experimental weight %	Theoretical weight %	Experimental atomic %	Theoretical atomic %
Oxygen (O)	31.67	22.48	29.32	12.37
Carbon (C)	50.71	65.51	62.54	48.07
Sulfur (S)	17.51	12.92	8.14	3.55

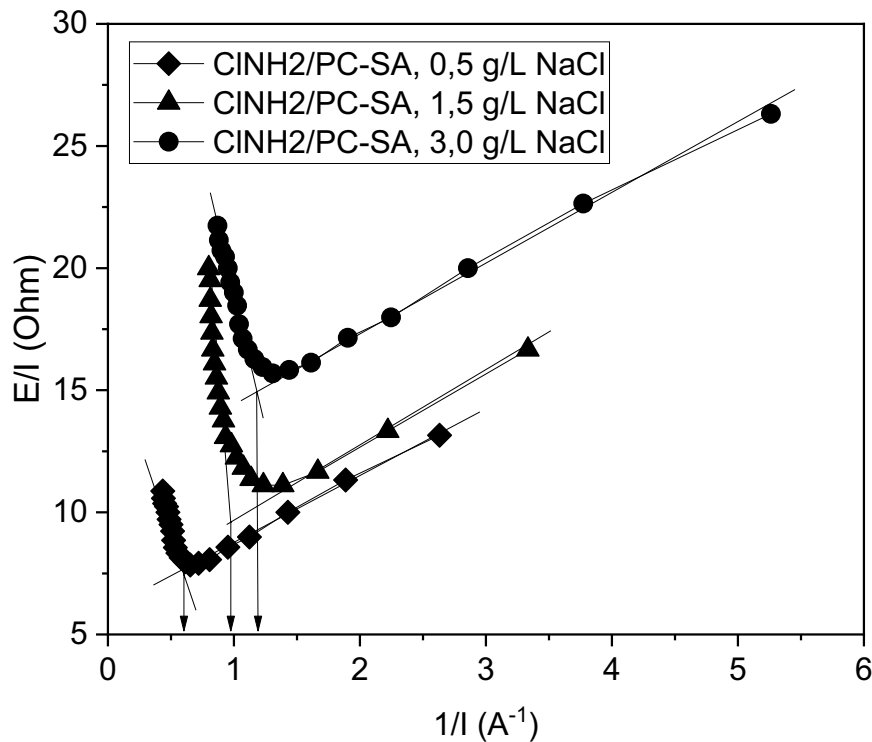


Fig. 4. Limiting the current of all assemblies with different solutions.

Table 3
Limiting current of all assemblies with different solutions

Fluorine content (mg/L)	3.00	3.00	3.00
NaCl concentration (g/L)	0.50	1.50	3.00
Limiting current density (mA/cm ²)	25.93	15.62	13.02
Debited current density (mA/cm ²)	20.78	12.50	10.41

The variation of conductivity in the dilute cell (DC) for both membranes, fabricated and commercial, is shown in Fig. 5. The general shape of the curves is reminiscent of a decrease of exponential shape. At low NaCl concentration, this pattern changes: the decrease in conductivity in the dilution compartment becomes more linear. The ionic composition would therefore influence the kinetics of the conductivity. We acknowledge that the NaCl conductivity in presence of fluoride in the dilute cell is reduced by increasing the desalination time for both membranes. All conductivity in the dilute tank for different concentration decrease in the same way. The conductivity of the dilute solution cell can be interpreted by the permeation of anions and cations through the AEM and CEM membranes under the applied electric field respectively. This is due to a significant decrease in ion concentration and to an increase in ionic diffusion resulting in molar conductivity decreasing in the dilute compartment.

Fig. 6 shows the voltage behavior throughout the ED experiment with CINH2 and PC-SA membranes during the ED experiments for the separation of fluorine. An exceptionally negligible voltage at the beginning of the ED experiment is observed. This is a direct consequence of the

absence of ion migration across the membrane and corresponds to the filling of the installation and to the activation polarization in the electrodes. Already after 1 min of operation, the voltage increases rapidly depending on the concentration of the feed solution. When the feed concentration increases the voltage decrease gradually.

The amount of fluoride in the dilute compartment of fluoride concentration and demineralization rate (DR) was determined and reported Fig. 7. The rapid defluoridation along with desalination was observed with all the varied initial feed concentrations.

Defluoridation and DR follow a rapid process due to the rapid mobility of ions with co-ions during desalination. At low NaCl concentration (0.5 g/L) the fluoride concentration reached the value of 0.2 mg/L after 25 min with is lower than the permissible limit. However, at higher concentrations, the 50% fluoride removal was reached within 10 min, and further as desalination proceeded the fluoride concentration decreased along and reached 0.1 mg/L and the demineralization rate can reach 95% after 45 min.

The fluoride removal experiment was conducted with fluoride paired only with sodium chloride (Fig. 8). The increase in chloride ions on the feed solution has not affected the removal rate of fluoride ions. Effectively and as depicted in Fig. 8 removal rate of fluoride increases more from these conditions. It is noticed that the fluoride removal, in the presence of monovalent ions was successfully carried out. The removal rate of fluoride of the least concentrated solution can achieve 90% after 25 min while the most concentrated solution (3 g/L) of NaCl can reach 97% after 45 min.

Fluoride removal depends on the initial salt concentration (Fig. 7). The most important observation is that the total

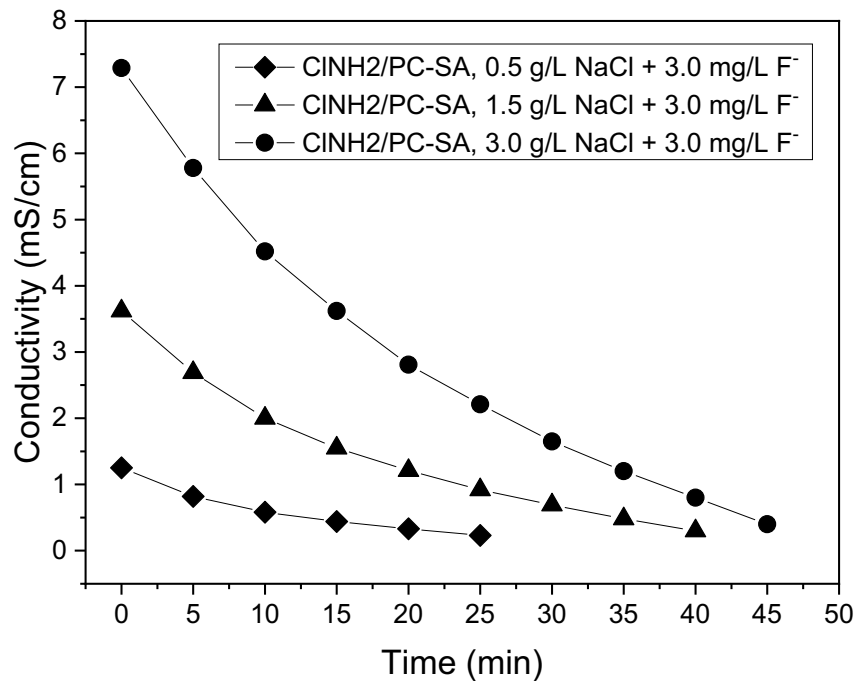


Fig. 5. Evolution of conductivity with a time of all assemblies in the dilute tank.

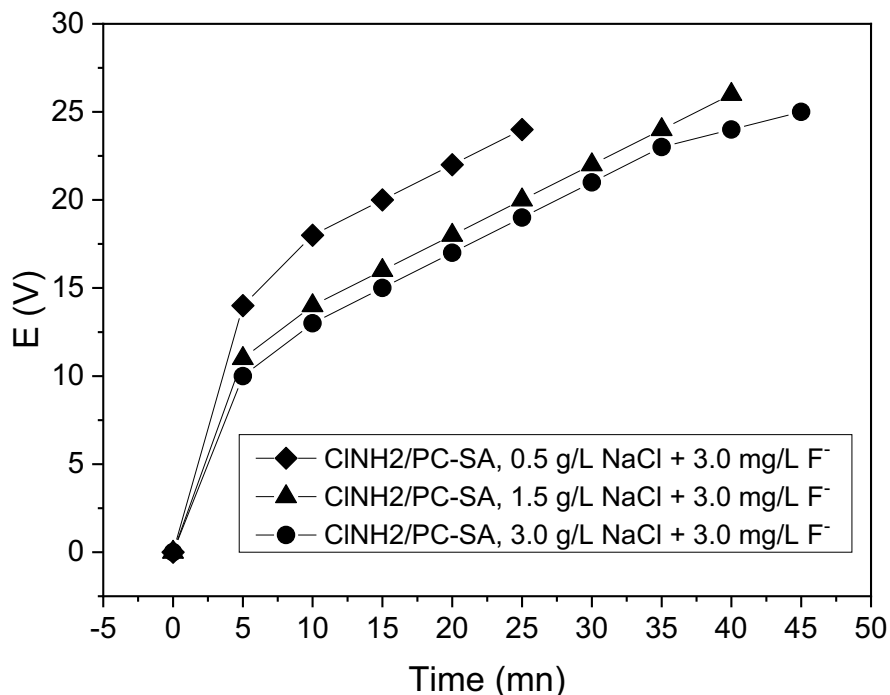


Fig. 6. Voltage is a function of the time during electro dialysis.

process time increased with an increasing initial concentration of the feed solution. This is can be explained by an increase in the ions rate of solutions when the concentration of salts increases. In other words, the treated solution could stay longer in the ED cell and the ions could be transferred freely across the membrane. Consequently, the ionic transport flux and specific power consumption depend on it, as

seen in Figs. 9 and 10. As a result, a competitive transfer can appear between fluoride ions and other ions (chloride ions in this case). The same results were demonstrated by Sadrzadeh et al. [38] and Sik Ali et al. [39].

Although the ionic flux is low, the performances of membranes in terms of flux are close to zero at the end of all experiments. These results are very encouraging of the

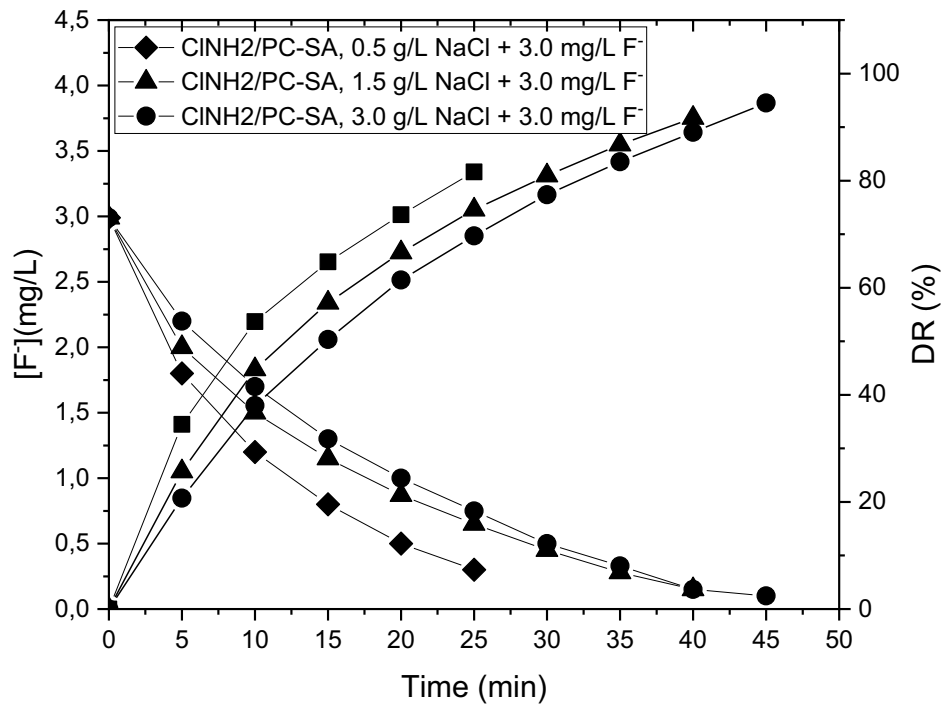


Fig. 7. Demineralization rate and fluoride removal of all assemblies.

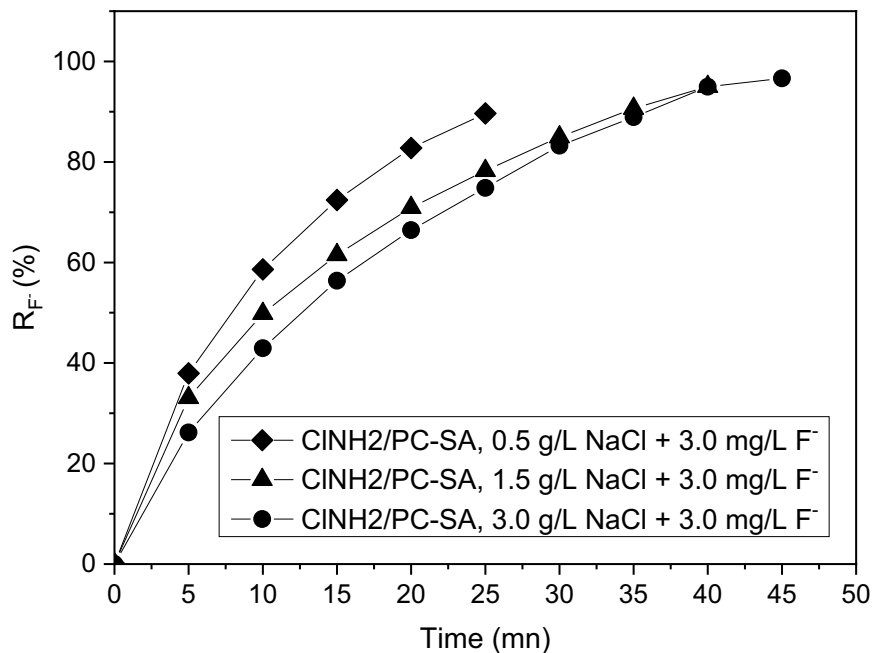


Fig. 8. The removal rate of fluoride ions using CINH2 membranes.

selective permeation of ions. The ionic flux decreases for all membranes but its decrease is lower for the solution of 0.5 g/L of NaCl (Fig. 9). A general trend for the three solutions is that the flux decreases drastically within 25 min and does not change significantly until the end of the experiments. It is noted that the starting fluxes are high but then decrease as a function of time before reaching zero and

stables values. For 0.5 and 1.5 g/L solutions, this stability is reached after 25 min. Whereas, for 3.0 g/L solution, the ionic flux vanishes after 35 min. This phenomenon can be related to the decrease in ionic entities within the dilute compartment [40].

The determination of the specific energy consumption ($W h L^{-1}$) provides good insight into the energy consumption of the used membranes stack. Fig. 10 summarizes the

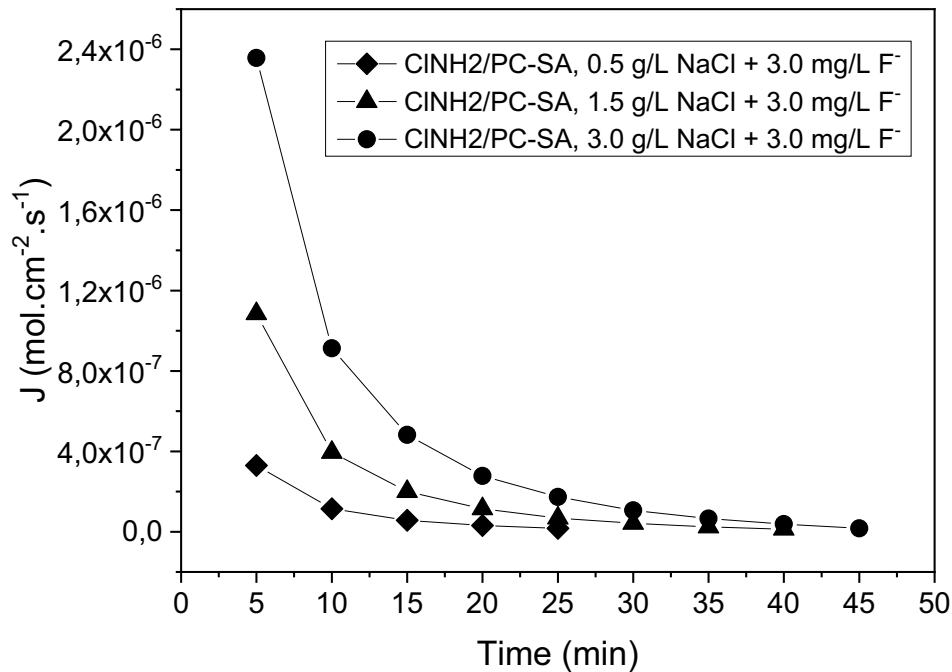


Fig. 9. Ionic transport flux.

SPC values calculated for various initial concentrations of sodium chloride and the fixed fluoride amount. The specific power consumption depends on the concentration of a treated solution and it is lower for low solution concentration. The SPC depends mainly on two parameters: the applied current and operation time. The applied current (debited current) is depending on the concentration as shown in Table 3. It is lower for low concentration. The operation time to obtain the same results (removal of 97% of fluoride) increased by increasing the concentration.

5. Conclusion

CINH2 membranes have been elaborated by chemical crosslinking of chlorosulfonated polyethersulfone (1.3 SO₂Cl pmu) with aminated polyethersulfone NH₂-PES and tested with commercial anionic membranes to check the correct functioning of electrodialysis during the fluoride removal. The micrograph SEM confirms the homogeneity of the synthesized CINH2 membrane and the absence of any cracks, holes or pores. The infrared analysis allowed us to have the characteristic peaks of functional groups of the CINH2 membrane. The results from the present study showed that the removal of fluoride was independent of the feed concentration solution. However, the initial concentration of the feed solution has a significant effect on the defluoridation efficiency and mainly on the demineralization rate and specific power consumption. The increase of the later parameter induced an increase in the energy needed to perform the required operation. As a result of the application of electrodialysis on the synthetic water sample, fluoride concentration could be reduced from 3.0 to 0.3 mg/L (97% removal), which is lower than the WHO standard (1.5 mg/L). Moreover, the concentration of different

species in the obtained treated water is below the amounts recommended by WHO for drinking water.

References

- [1] M. Vasselbehagh, H. Karkhanechi, S. Mulyati, R. Takagi, H. Matsuyama, Improved antifouling of anion-exchange membrane by polydopamine coating in electrodialysis process, *Desalination*, 332 (2014) 126–133.
- [2] S.M. Hosseini, A. Gholami, S.S. Madaeni, A.R. Moghadassi, A.R. Hamidi, Fabrication of (polyvinyl chloride/cellulose acetate) electrodialysis heterogeneous cation exchange membrane: characterization and performance in desalination process, *Desalination*, 306 (2012) 51–59.
- [3] A.H. Galama, G. Daubaras, O.S. Burheim, H.H.M. Rijnaarts, J.W. Post, Seawater electrodialysis with preferential removal of divalent ions, *J. Membr. Sci.*, 452 (2014) 219–228.
- [4] R.K. Nagarale, G.S. Gohil, V.K. Shahi, Recent developments on ion-exchange membranes and electro-membrane processes, *Adv. Colloid Interface Sci.*, 119 (2006) 97–130.
- [5] C. Vogel, J. Meier-Haack, Preparation of ion-exchange materials and membranes, *Desalination*, 342 (2014) 456–474.
- [6] J. Tang, L. Wan, Y. Zhou, L. Ye, X. Zhou, F. Huang, Synthesis and performance study of a novel sulfonated polytriazole proton exchange membrane, *J. Solid State Electrochem.*, 21 (2017) 725–734.
- [7] M.I. Khan, Ch. Zheng, A.N. Mondal, Md.M. Hossain, B. Wu, K. Emmanuel, L. Wu, T. Xu, Preparation of anion exchange membranes from BPPO and dimethylethanolamine for electrodialysis, *Desalination*, 402 (2017) 10–18.
- [8] J. Ran, L. Wu, Y. He, Z. Yang, Y. Wang, Ch. Jiang, L. Ge, E. Bakangura, T. Xu, Ion exchange membranes: New developments and applications, *J. Membr. Sci.*, 522 (2017) 267–291.
- [9] Ch. Klaysom, R. Marschall, L. Wang, B.P. Ladewig, G.Q.M. Lu, Synthesis of composite ion-exchange membranes and their electrochemical properties for desalination applications, *J. Mater. Chem.*, 20 (2010) 4669–4674.
- [10] M.P. Hamedani, Sh.M. Ataei, Effect of sulfonation degree on molecular weight, thermal stability, and proton conductivity

- of poly(acetylene ether sulfone)s membrane, Des. Monomers Polym., 20 (2016) 54–65.
- [11] T. Luo, S. Abdu, M. Wessling, Selectivity of ion exchange membranes: a review, J. Membr. Sci., 555 (2018) 429–454.
- [12] W. Mabrouk, L. Ogier, F. Matoussi, C. Sollogoub, S. Vidal, M. Dachraoui, J.F. Fauvarque, Preparation of new proton exchange membranes using sulfonated poly(ether sulfone) modified by octylamine (SPESOS), Mater. Chem. Phys., 128 (2011) 456–463.
- [13] L. Hao, J. Liao, Y. Liu, H. Ruan, A. Sotto, B.V. Bruggen, J. Shen, Highly conductive anion exchange membranes with low water uptake and performance evaluation in electrodialysis, Sep. Purif. Technol., 211 (2019) 481–490.
- [14] Ch. Olkis, S. Brandani, G. Santori, Design and experimental study of a scale adsorption desalinators, Appl. Energy, 253 (2019) 113584, doi: 10.1016/j.apenergy.2019.113584.
- [15] K. Hwang, J.H. Kim, S.Y. Kim, H. Byun, Preparation of polybenzimidazole-based membranes and their potential applications in the fuel cell system, Energies, 7 (2014) 1721–1732.
- [16] R. Ullah, M.S. Zafar, N. Shahani, Potential fluoride toxicity from oral medicaments: a review, Iran J. Basic Med. Sci., 20 (2017) 841–848.
- [17] A. Rasool, A. Farooqi, T. Xiao, W. Ali, S. Noor, O. Abiola, S. Ali, W. Nasim, A review of global outlook on fluoride contamination in groundwater with prominence on the Pakistan current situation, Environ. Geochem. Health, 40 (2018) 1265–1281.
- [18] Z. Luo, D. Wang, D. Zhu, J. Xu, H. Jiang, W. Geng, W. Wei, Z. Lian, Separation of fluoride and chloride ions from ammonia-based flue gas desulfurization slurry using a two-stage electrodialysis, Chem. Eng. Res. Des., 147 (2019) 73–82.
- [19] A. Bhatnagar, E. Kumar, M. Sillanpaa, Fluoride removal from water by adsorption – a review, Chem. Eng. J., 171 (2011) 811–840.
- [20] H. Huang, J. Liu, P. Zhang, D. Zhang, F. Gao, Investigation on the simultaneous removal of fluoride, ammonia nitrogen and phosphate from semiconductor wastewater using chemical precipitation, Chem. Eng. J., 307 (2017) 696–706.
- [21] L.F. Castaneda, J.F. Rodriguez, J.L. Nava, Electrocoagulation as an affordable technology for decontamination of drinking water containing fluoride: a critical review, Chem. Eng. J., 431 (2021) 67–84.
- [22] N. Arahman, S. Mulyati, M.R. Lubis, R. Takagi, H. Matsuyama, The removal of fluoride from water based on applied current and membrane types in electrodialysis, J. Fluorine Chem., 191 (2016) 97–102.
- [23] M. Ameer, F.H. Azaza, L.B. Cheikha, M. Gueddari, Geochemistry of high concentrations of fluoride in groundwater at Oued Rmel aquifer (North-eastern Tunisia), and risks to human health from exposure through drinking water, Environ. Earth Sci., 184 (2019) 1–9.
- [24] J. Fito, H. Said, S. Feleke, A. Worku, Fluoride removal from aqueous solution onto activated carbon of *Catha edulis* through the adsorption treatment technology, Environ. Syst. Res., 8 (2019) 1–10.
- [25] W. Mabrouk, L. Ogier, C. Sollogoub, S. Vidal, F. Matoussi, J.F. Fauvarque, Synthesis and characterization of new membranes deriving from sulfonated polyethersulfone for PEMFC applications, Desal. Water Treat., 56 (2015) 2637–2645.
- [26] W. Mabrouk, L. Ogier, S. Vidal, C. Sollogoub, F. Matoussi, J.F. Fauvarque, Ion exchange membranes based upon crosslinked sulfonated polyethersulfone for electrochemical applications, J. Membr. Sci., 452 (2014) 263–270.
- [27] W. Mabrouk, R. Lafi, J.F. Fauvarque, A. Hafiane, C. Sollogoub, New ion exchange membrane derived from sulfochlorated polyether sulfone for electrodialysis desalination of brackish water, Polym. Adv. Technol., 32 (2020) 1–11.
- [28] J. Kerres, W. Zhang, W. Cui, New sulfonated engineering polymers via the metalation route. II. Sulfinated/sulfonated poly(ether sulfone) PSU Udel and its crosslinking, J. Polym. Sci. Polym. Chem., 36 (1998) 1441–1448.
- [29] S. Thampy, G.R. Desale, V.K. Shahi, B.S. Makwana, P.K. Ghosh, Development of hybrid electrodialysis-reverse osmosis domestic desalination unit for high recovery of product water, Desalination, 282 (2011) 104–108.
- [30] D.A. Cowan, J.H. Brown, effect of turbulence on limiting current in electrodialysis cells, Ind. Eng. Chem. Res., 51 (1959) 1445–1448.
- [31] V. Geraldes, M.D. Afonso, Limiting current density in the electrodialysis of multi-ionic solutions, J. Membr. Sci., 360 (2010) 499–508.
- [32] M.L. Cerva, L. Gurreri, M. Tedesco, A. Cipollina, M. Ciofalo, A. Tamburini, G. Micale, Determination of limiting current density and current efficiency in electrodialysis units, Desalination, 455 (2018) 138–148.
- [33] W. Villeneuve, V. Perreault, P. Chevallier, S. Mikhaylin, L. Bazinet, Use of cation-coated filtration for demineralization by electrodialysis, Sep. Purif. Technol., 218 (2019) 70–80.
- [34] W.D. Schepper, M.D. Moraru, B. Jacobs, M. Oudshoorn, J. Helsen, Electrodialysis of aqueous NaCl-glycerol solutions: a phenomenological comparison of various ion exchange membranes, Sep. Purif. Technol., 217 (2019) 274–283.
- [35] A. Al-Jubainawi, Z. Ma, Y. Guo, L.D. Nghiem, Effect of regulating main governing factors on the selectivity membranes of electrodialysis used for LiCl liquid desiccant regeneration, J. Build. Eng., 28 (2020) 1–34.
- [36] X. Wang, N. Li, J. Li, J. Feng, Z. Ma, Y. Xu, Y. Sun, D. Xu, J. Wang, X. Gao, J. Gao, Fluoride removal from secondary effluent of the graphite industry using electrodialysis: optimization with response surface methodology, Front. Environ. Sci. Eng., 51 (2019) 1–11.
- [37] H. Lee, H. Strathmann, S.H. Moon, Determination of the limiting current density in electrodialysis as an empirical function of linear velocity, Desalination, 190 (2006) 43–50.
- [38] M. Sadzadeh, A. Ramzi, T. Mohammadi, Separation of different ions from wastewater at various operating conditions using electrodialysis, Sep. Purif. Technol., 54 (2007) 147–156.
- [39] M.B. Sik Ali, B. Hamrouni, M. Dhahbi, Electrodialytic defluoridation of brackish water: effect of process parameters and water characterization, Clean–Soil Air Water, 38 (2010) 623–629.
- [40] C. Evangeline, V. Pragasan, K. Rambabu, S. Velu, P. Monash, G. Arthanareeswaran, F. Banat, Iron oxide modified polyethersulfone/cellulose acetate blend membrane for enhanced defluoridation application, Desal. Water Treat., 156 (2019) 177–188.